Earth Science Research; Vol. 13, No. 1; 2024
ISSN 1927-0542 E-ISSN 1927-0550
Published by Canadian Center of Science and Education

Mechanical Microdeformation and Kink–band Formation in Mica from the Colônia Impact Crater, São Paulo, Brazil

Victor F. Velázquez[1], José M. Azevedo Sobrinho[2], Rodrigo F. Lucena[1], Alethéa E. M. Sallun[2] & William Sallun Filho[2]

[1] School of Arts, Sciences, and Humanities, University of São Paulo, Arlindo Béttio, 1000, CEP 03828-000, São Paulo, Brazil

[2] Environmental Research Institute, Secretariat for the Environment, Infrastructure and Logistics, Joaquim Távora, 822, CEP 04015-011, São Paulo, Brazil

Correspondence: Victor F. Velázquez, School of Arts, Sciences, and Humanities, University of São Paulo, Arlindo Béttio, 1000, CEP 03828-000, São Paulo, Brazil. Tel: 11 55 30918150. E-mail: vvf@usp.br

Received: September 4, 2024 Accepted: October 8, 2024 Online Published: October 22, 2024

doi:10.5539/esr.v13n1p1 URL: https://doi.org/10.5539/esr.v13n1p1

Abstract

A comprehensive examination using a transmitted light optical microscope was conducted to analyze the morphology and geometric parameters of kink band development in mica from the Colônia impact crater's crystalline basement rocks. Significant differences were observed between kink bands formed perpendicular and parallel to the [001] plane. Kink bands perpendicular to the [001] are narrow and elongated, exhibiting two distinct coplanar orientations with regular spacing and parallel planar fractures, which suggest a slip-dislocation strain mechanism. In contrast, kink bands parallel to the [001] plane exhibit a greater variety of shapes and a more complex internal structure. These kink bands can be grouped into six types: sigmoidal-shape, S-shape, lenticular-shape, Z-shape, Z-shape with internal dislocation, and Z-shape with internal rotation. The deformation patterns in these kink bands indicate two primary processes: flexural and shear strain. The most notable deformations induced by these strain mechanisms include the curvature of cleavage lamellae, delamination cracks, and fractures along the boundaries of kink bands. More severely deformed kink bands exhibit dislocation, rotation, and partial obliteration of internal cleavage lamellae. These characteristics differ from those of typical kink bands in tectonically deformed rocks, thereby reviving the longstanding debate regarding their potential use as alternative evidence in impact cratering investigations.

Keywords: kink band, mica, microdeformation, Colônia impact crater

1. Introduction

An impact structure or crater forms when asteroids or comets collide with a planet or moon, resulting in a circular depression with a raised rim (Melosh and Ivanov, 1999). The impact generates extreme thermodynamic conditions, converting the bolide's kinetic energy into powerful shock waves that radiate outward from the point of contact. As the shock wave propagates through the target material, a bowl-shaped cavity forms and a variety of shock metamorphism features develop (French, 1998). Notable irreversible changes include shatter cones, planar deformation features, kink bands in minerals, high-pressure metamorphic minerals, small holohyaline natural objects, and melting-bearing rocks (French, 1998; Osinski and Pierazzo, 2012).

The Colônia Crater is located 40 km from São Paulo's city center, at coordinates 23˚52'27"S and 46˚42'36"W, in the Parelheiros district. This ring-like depression (Fig. 1B), with a diameter of 3.6 km, is the most prominent geomorphological feature in the region (Koller et al., 1961). It is characterized by a smooth bowl shape and a 120 m difference in relief between the rim and the floor (Riccomini et al., 2005). The crater developed within an important orogenic zone known as the Ribeira Fold Belt (Hasui et al., 1975). In the study area, this regional geological domain can be divided into three main lithostratigraphic units (Fig. 1C): (a) the Precambrian crystalline basement, which includes granite, granodiorite, mica schist, gneiss, and migmatite; (b) Tertiary siliciclastic sediments, correlating with the Resende Formation; and (c) Quaternary deposits that cover much of the crater and consist of alternating psammitic and organo-pelitic layers (Coutinho, 1980; Riccomini et al., 2005).

Over the last ten years, numerous samples from the Colônia impact crater's allochthonous breccia deposits have been subjected to detailed petrographic examination. These studies have revealed a set of distinctive shock-metamorphic features, including planar deformation features in quartz, kink bands in mica, ballen silica, and granular texture in zircon (Velázquez et al., 2013). Additionally, a wide variety of impact-melt-bearing rocks have been identified (Velázquez et al., 2018), along with spherules of heterogeneous composition resulting from melting and vaporization products (Velázquez et al., 2021).

Kink bands are common in geological materials, whether present in large-scale strata or in single crystals (Hörz and Ahrens, 1969). The earliest descriptions of kinking in kyanite and mica from tectonically deformed rocks are attributed to Becke (1892) and Mügge (1898), respectively. Since then, kink bands have been reported in rocks formed during regional metamorphism (Turner, 1964) and in those deformed by asteroid impacts (Stöffler, 1966). The formation mechanism can vary significantly and is largely influenced by the crystalline glide plane (Christoffersen and Kronenberg, 1993) and the stress regime to which the mineral has been subjected (Etheridge et al., 1973).

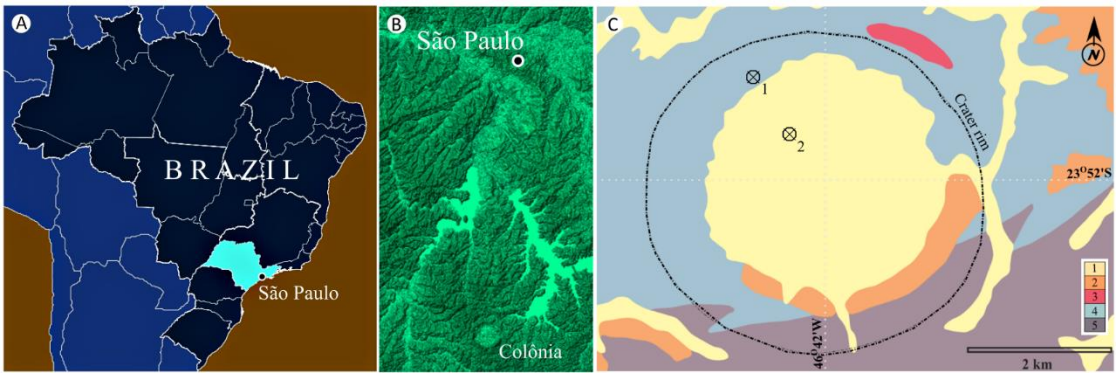

Figure 1. A) Location of São Paulo city. B) The Colônia impact crater within the São Paulo metropolitan region. C) Schematic geological map of the Colônia impact crater region (Riccomini et al., 2005). Legend: 1 - Quaternary alluvial deposits, 2 - Tertiary sediments, 3 - Diorite and quartz diorite, 4 - Mica schist and quartzite, 5 - Gneiss and migmatite. The drillholes, ⊗1 and ⊗2, are according to Velázquez et al. (2021)

Due to its common occurrence in various geological processes and its wide range of morphological aspects, a detailed analysis was performed using a transmitted light optical microscope to examine the primary morphological features of kink bands developed under extreme P-T conditions. These kink bands, documented by Velázquez et al. (2013) in mica from crystalline basement rocks that have experienced varying degrees of shock metamorphism, are the focus of this study that aims to thoroughly evaluate the morphology and underlying processes contributing to the formation of these kink bands, based on recent theoretical formulations.

2. Brief Conceptual Approach

2.1 Structural Features of Mica

The mica group includes six mineral species, but only muscovite and biotite are common enough to be found in igneous, sedimentary, and metamorphic rocks. These micas are part of the broader category of rock-forming silicate minerals known as phyllosilicates. Phyllosilicates are characterized by a fundamental building block: a two-dimensional layer of silicon-oxygen tetrahedra (SiO_4) arranged in a sheet-like structure (Deer et al., 2013). This structure features a three-layer arrangement of tetrahedral (T) and octahedral (O) interconnections, forming a distinctive 2:1 layer (Fig. 2).

Many of mica's specific properties are attributed to its two-dimensional sheet layer structure. For example, the strong covalent bonds in the tetrahedral and octahedral layers provide strength and flexibility. On the other hand, mica's exceptional cleavage results from weak electrostatic forces between its layers, allowing the sheets to glide easily over one another. (Ferraris and Ivaldi, 2002; Deer et al., 2013).

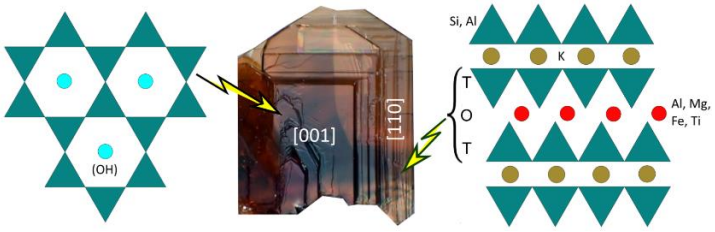

Figure 2. Schematic representation of mica structure based on Klein and Hurlbut (1993). The biotite crystal image was obtained from the homepage of mindat.org

2.2 Kink Band Formation Mechanism

In the fields of geology and materials science, kink bands are characterized by abrupt changes in deformation direction, which distinguish them from the surrounding undeformed areas (Anderson, 1964). Laboratory deformation experiments have shown that kink bands can progressively thicken and reorient as deformation increases. The evolution of kink bands is a dynamic process characterized by complex interactions between a mineral's crystalline structure and the surrounding stress field (Pimenta et al., 2009). This phenomenon is particularly common in materials subjected to compressive stress, especially those with pronounced anisotropic properties (Peterson and Weiss, 1966). Anisotropy is characterized by discrepancies in a material's properties, which may involve the orientation, distribution, or composition of its individual phases.

Although kinking occurs in various metals and rock-forming minerals, it is particularly prominent in layer-structured minerals such as muscovite and biotite (Hörz and Ahrens, 1969). Advanced microscopy techniques have revealed the microstructural mechanisms underlying kink band formation, highlighting the significant roles of temperature and pressure in this process (Mares and Kronenberg, 1993). Elevated temperatures increase dislocation mobility, facilitating the formation of kink bands under lower stress conditions. Similarly, elevated pressures can influence both the thickness and orientation of kink bands, as high-pressure conditions typically result in more pronounced and widely spaced kink bands. According to Christoffersen and Kronenberg (1993), the initial phase of a kink band is induced by the displacement of atoms, which triggers the emergence of glide planes and other structural defects that exceed the deformation limit of layers or lamellae under high shear stress. The propagation of kinking through the material is governed by its anisotropic properties, as this specific region offers less physical resistance to deformation compared to the surrounding matrix (Wadee and Edmunds, 2005). In a simplified form, kink bands represent a new local arrangement of the material's internal structure induced by high stress.

3. Material and Methods

The 2D images of mica were captured using a high-resolution digital camera from a collection of 200 thin sections previously examined by Velázquez et al. (2013, 2018, 2021). Common distinctive morphological features used to characterize kink bands—such as shape, width, spacing, and orientation (Fig. 3)—are defined according to Verbeek (1978). For a more comprehensive analysis of the formation process, 50 azimuth measurements were taken for each parameter along a single reference plane using Levenhuk Toupview software. The azimuthal variation of each class was then depicted on rose diagrams with three different colors using RockWorks software.

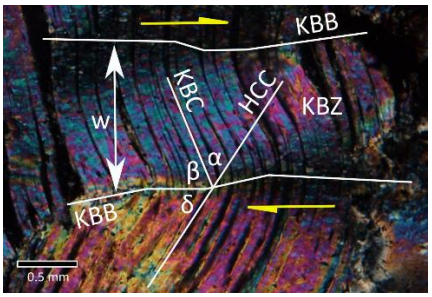

Figure 3. Geometric parameters of kink bands according to Verbeek (1978). KBZ represents the kink band zone; W denotes the kink band width; KBB refers to the kink band boundary; HCC is the host crystal cleavage; KBC indicates the internal cleavage of the kink band; α is the angle between HCC and KBC; β is the internal rotation angle of KBC; δ is the external angle of HCC. The yellow arrows indicate the overall sense of movement

4. Kink band Description and Characterization

The formation of kink bands has been extensively studied across various materials and scales, both in controlled laboratory conditions and natural settings (Misra and Burg, 2012; Anderson et al., 2021; Aller et al., 2020). However, the formation mechanism under extreme thermodynamic conditions, such as those involved in impact cratering, has received very little attention. In light of this, a detailed examination of individual grains—primarily muscovite and, to a lesser extent, biotite—from samples collected from the Colônia impact crater was conducted using a transmitted light microscope. These minerals are essential components of the crystalline basement rocks exposed in the area, which mainly consist of mica-rich quartzite, granite, granodiorite, and mica schist. In both igneous and strongly foliated metamorphic rocks, the thin individual plates of mica are well-preserved, showing no evidence of recrystallization, grain size reduction, or fish structures, which are typically observed in regional metamorphic terrains. However, microstructures induced by shock metamorphism have been extensively documented by Velázquez et al. (2013, 2018). The most common features include opacification of the edges, partial cleavage obliteration, and parallel planar fractures.

Although muscovite and biotite may exhibit different responses to stress, two distinct deformation conditions can be characterized. In some cases, strain occurs perpendicular to the basal plane of the mineral, while in other instances, it appears parallel to the cleavage plane. When the maximum stress acts perpendicular to the [001] direction, kink bands typically appear as narrow linear bands with wider spacing, often resembling elongated cones (Fig. 4A). In certain cases, these kink bands are arranged in two distinct orientations, resulting in a prominent X-intersection (Fig. 4A). The angle formed by this intersection typically ranges between 40º and 50º. The propagation of the bands beyond the intersection suggests that they developed in response to stress regimes acting at different intervals and in two main directions. Along these kink bands, small en-echelon dislocations and plane-parallel fractures are also common. These fractures are very thin, markedly short, and symmetrically arranged at angles ranging from 30° to 40° relative to the major axis of the kink bands (Figs. 4A and 4B).

Strains occurring parallel to the cleavage plane have led to the formation of kink bands with notable microstructural features. These kink bands vary significantly but are fundamentally characterized by closely spaced, parallel or semi-parallel linear boundaries, irregular widths, and complex intersections (Fig. 4C). The intricate patterns observed often result from the interplay of these features, creating a distinctive and complex microstructural arrangement.

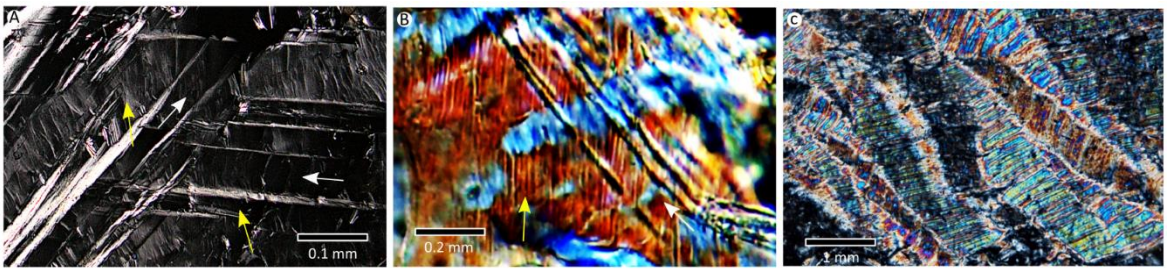

Figure 4. The morphology of kink bands varies depending on the orientation of the crystallographic plane. Muscovite (A) and biotite (B) exhibit strain perpendicular to the [001] plane, with the orientation of kink bands and associated planar fractures indicated by white and yellow arrows, respectively. Muscovite with strain parallel to the [001] plane displays a wide variety of kink bands (C)

Considering both the morphological features and internal frameworks, six distinct types of predominant shapes were identified from the analysis of 200 mica grains (Fig. 5). Although there is no intention to establish rigid classification rules, the distinction between these shapes will be maintained in the following sections to effectively highlight the most important aspects of the description.

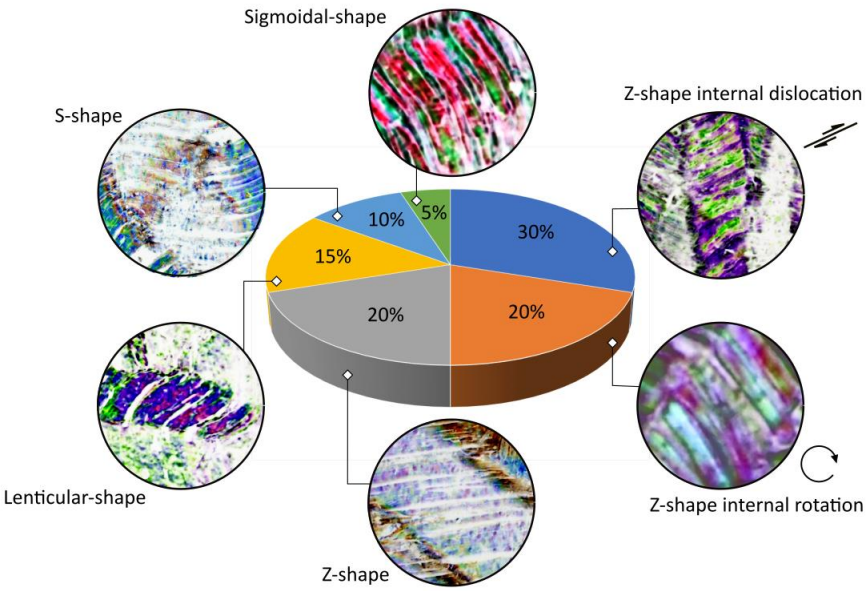

Figure 5. Frequency of the most common kink band morphologies determined from 200 individual mica grains. A negative filter was applied to enhance image contrast

4.1 S-shape

The vast majority of S-shape kink bands display broadly curved boundaries, with delamination cracks occurring at the maximum point of curvature (Fig. 6A). These kinks typically exhibit a large deformation zone (KBZ), ranging from 1.28 mm to 2.03 mm. Pervasive delamination cracks, which show noticeable curvilinear expansion, and partial obliteration of the cleavage lamellae are common within the KBZ (Fig. 6A). The angles α and β often differ slightly, fluctuating within ranges of 47° to 49° and 55° to 58°, respectively (Fig. 6B). The recorded values for δ diverge significantly from these measurements, ranging from 73° to 75°. The rotation of HCC and KBC is clearly divergent, resulting in kink bands with asymmetrical morphology and an open interlimb angle.

4.2 Sigmoidal-shape

These kink bands display various distinctive features. Notable examples include a broad deformation zone (KBZ), ranging from 1.73 to 1.97 mm, and a subtle curvature in the cleavage lamellae (Fig. 6C). Delamination cracks occur less frequently (Fig. 6C), and no difference in the thickness of cleavage lamellae between HCC and KBZ was observed. The values of α exhibit minor fluctuations, ranging from 19° to 21° (Fig. 6D). In contrast, the angles β and δ show a marked increase, with β varying from 77° to 79° and δ from 83° to 85°. Notably, there is a strong correlation between these two angles. The data indicate significant rotation of the cleavage lamellae along the KBB (Fig. 6D), which is further corroborated by the pronounced gentle interlimb angle and the asymmetrical morphology of the kink bands.

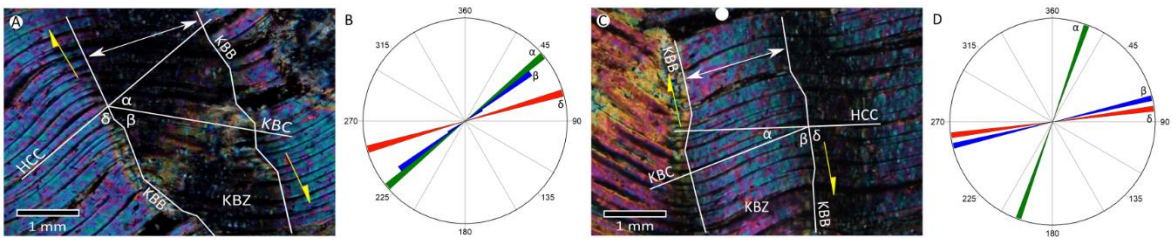

Figure 6. Morphological aspects of S-shape (A) and sigmoidal-shape (C) kink bands. Rose diagrams (B and D) illustrate the orientation patterns of the geometric parameters. Dark shadows between cleavage lamellae indicate delamination cracks

4.3 Z-shape

The Z-shape kink bands exhibit several notable distinguishing features. In the HCC and KBZ, the cleavage

lamellae are characterized by uniform thickness and a notable lack of curvature. Additional features include fractures that may occur on either or both sides of the KBB (Fig. 7A), minimal variations in KBZ (ranging from 0.90 mm to 1.05 mm) but with a large number of delamination cracks, and significant rotation of the cleavage lamellae, with α values between 21° and 23° (Fig. 7B). Most fractures have well-defined contours, although some are incipient and discontinuous. The angles β and δ, ranging from 49° to 53° and 73° to 75°, respectively, indicate significant rotation of the cleavage lamellae along the KBB (Fig. 7B). This variation, with inner angles (β > 45°) and outer angles (δ > 70°) of the cleavage lamellae (Fig. 7B), often results in an open interlimb angle and contributes to the asymmetric morphology of the kink bands.

4.4 Lenticular-shape

A notable feature of lenticular-shape kink bands is the presence of thicker cleavage lamellae, often accompanied by a significant occurrence of delamination cracks. These cracks are characterized by lateral expansion ranging from 0.03 mm to 0.08 mm (Fig. 7C). The KBZ has a width between 0.48 mm and 0.58 mm, and its boundaries are defined by continuous parallel linear fractures. The cleavage lamellae observed in the KBZ exhibit larger spacing, a smooth curvature, and a configuration resembling an elongated parallelogram with stretched ends (Fig. 7C).

Two important aspects concerning the host crystal are worth noting: firstly, a series of thin fractures cut the cleavage lamellae diagonally, displacing them in an en-echelon pattern; secondly, in areas close to the KBBs, the cleavage lamellae are generally obliterated (Fig. 7C). The angles α (48°-51°) and δ (59°-61°) show a strong correspondence, in contrast to the relatively high angles β (73°-75°) (Fig. 7D). This high angular ratio, as observed in other kink bands, contributes to an open interlimb angle and asymmetric morphology.

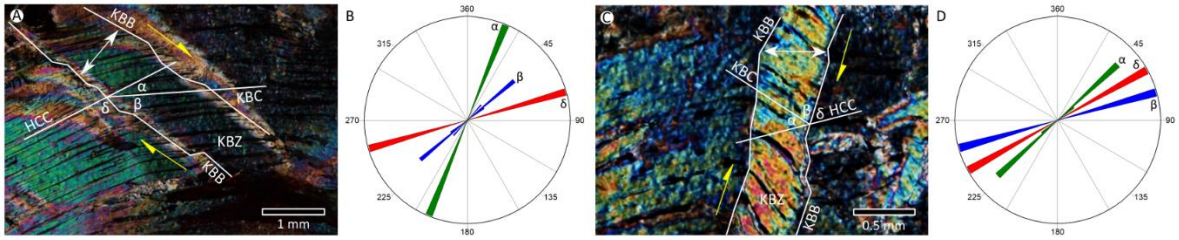

Figure 7. Morphological aspects of Z-shape (A) and lenticulars-shape (C) kink bands. Rose diagrams (B and D) illustrate the orientation patterns of the geometric parameters. In (A), a homogeneous displacement in the dextral sense is observed in the internal lamellae. In (C), the cleavage lamellae in the host crystal are partially obliterated, while in the KBZ they show curvatures and stretched ends

4.5 Z-shape Internal Dislocation

The Z-shape internal dislocation kink bands (Fig. 8A) generally exhibit high external and internal rotation angles of the cleavage lamellae, with α, β, and δ ranging from 57° to 60°, 64° to 66°, and 53° to 55°, respectively (Fig. 8B). The variation in rotation angles results in a distinctive feature of these kink bands: asymmetric morphology. This configuration highlights the complex organization of the internal structure of the lamellae.

The KBZ is characterized by a width ranging from 0.25 mm to 0.38 mm, continuous linear fractures, and notable differences in cleavage lamellae. In the KBZ, the lamellae are thicker and exhibit a pronounced tendency toward en-echelon dislocations, whereas in the host crystal, they are thin, uniform, and continuous (Fig. 8A). Despite the significant discrepancy in the configuration and dimensions of the cleavage lamellae, no curvature was observed. In some instances, the network of interconnected lamellae in the KBZ exhibits parallel dislocations, resulting in a domino-like pattern (Fig. 8A). The open interlimb angle and asymmetric morphology are attributed to the differing rotation patterns between the cleavage lamellae of the HCC and KBC.

4.6 Z-shape Internal Rotation

The Z-shape internal rotation kink bands exhibit considerable variation in width, ranging from thin (0.17 mm) to relatively thick (0.42 mm) (Fig. 8C). These kink bands also show high rotation angles, with α and β values ranging from 41° to 43° and 73° to 75°, respectively (Fig. 8D). The thickness of the cleavage lamellae varies along the KBZ: thinner lamellae are more common in the narrower segments, while thicker lamellae are predominant in the wider segments. In both cases, the ends of the lamellae near the KBB exhibit curvature.

Another important aspect to consider is the extinction angle of the thin cleavage lamellae in the KBZ. Although the displacement of the lamellae along the plane generally aligns with the predominant direction of movement,

noticeable divergences in both the magnitude and direction of rotation are observed when the microscope stage is rotated. These divergences can occur in either a clockwise or counterclockwise direction (Fig. 8C). The open interlimb angle is more common, although small variations can also be observed.

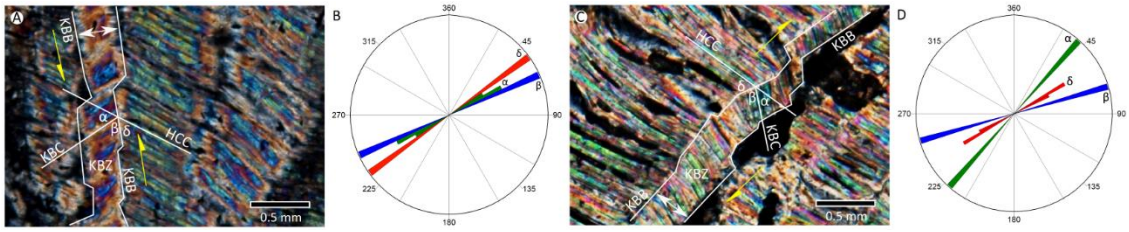

Figure 8. Morphological aspects of Z-shape internal dislocation (A) and Z-shape internal rotation (C) kink bands. Rose diagrams (B and D) illustrate the orientation patterns of the geometric parameters. In (A), the lamellae in the KBZ display a domino pattern and a dextral dislocation component. In (C), the overlapping thin lamellae with varying extinction angles in the KBZ indicate an internal clockwise rotation

5. Discussion on Stress-strain and Kink band Formation

A comprehensive examination of individual muscovite and biotite grains revealed a wide range of sharply defined kink bands in both planes: those parallel and those perpendicular to [001]. Kink bands that formed perpendicular to the [001] plane are clearly separated from each other and exhibit an elongated, narrow shape, with minimal morphological variations. Across all examined samples, coplanar kink bands are arranged into two distinct sets, each displaying different orientation patterns. Although determining the precise temporal relationship between these orientation patterns can be challenging in some cases, their notable morphological similarity suggests that these coeval kink bands developed under similar strain conditions. However, slight fluctuations in the direction of deviatoric stress over relatively short time intervals may have occurred.

The intricate patterns of arrangement, orientation, and distribution imply that a complex mechanism involving slip-displacement processes played a significant role in the development of the kink bands. As extensively documented by Bell et al. (1986), Kronenberg et al. (1990), and Christoffersen and Kronenberg (1993), this process involves the removal of individual atoms or small groups of atoms from specific discontinuities within the crystalline structure, which are then transferred to other interfaces in response to applied stress, resulting in visible physical changes in the mineral. When compressive stress is applied under high pressure and temperature conditions, such as in an impact crater, the movement of atoms and the rearrangement of the crystal lattice are facilitated. High temperature provides thermal energy that reduces resistance to movement, while high pressure allows the relative sliding of atomic layers within the crystal structure. Consequently, the dislocation of part of the crystalline structure leads to the formation of narrow parallel kink bands.

Associated with this strain type, numerous minor features were detected, notably the presence of several parallel fine fractures that are either adjacent to or intersecting the kink bands. These features are interpreted as potential ladder structures.

The kink bands parallel to the [001] plane exhibit numerous distinctive features. Most of these bands have well-defined boundaries and display a wide range of shapes and sizes, with significant variations in geometric parameters and complex deformation of the cleavage lamellae (Fig. 9). These observations suggest substantial fluctuations in the local stresses to which the mica grains were subjected, particularly concerning the orientation and intensity of the maximum stress relative to the cleavage plane of the mineral. Despite the presence of unusual morphological elements and differing pressure and temperature conditions compared to those typically replicated in laboratory settings or found in regional metamorphism, the kink bands reported in this study share primary characteristics with the experimental models described by Twiss and Moores (2007), Misra and Burg (2012), and Plummer et al. (2021). Notable features of these bands include a sharp change in cleavage orientation relative to its original position, deformation within a well-defined band, and a reduction in the spacing of layers within the kink band.

Kink band morphology	Geometric parameters			Boundary	Width (mm)	Interlimb angle	Kink band zone features	Strain
	α	β	δ					
Sigmoidal-shape	19°-21°	77°-79°	83°-85°	No evidence of fractures	1.73-1.97	Gentle	Cleavage lamellae with gentle curvature and delamination crack	Flexural
S-shape	47°-49°	55°-58°	73°-75°	No evidence of fractures	1.28-2.03	Open	Cleavage lamellae with strong curvature and delamination crack	Flexural
Lenticular-shape	48°-51°	73°-75°	59°-61°	Delimited by fractures	0.48-0.58	Open	Cleavage lamellae with stretched ends	Shear
Z-shape	21°-23°	49°-53°	73°-75°	Delimited by fractures	0.90-1.05	Open	Cleavage lamellae with uniform parallel displacement.	Shear
Z-shape internal dislocation	57°-60°	64°-66°	53°-55°	Delimited by fractures	0.25-0.38	Open	Cleavage lamellae with parallel en-echelon pattern dislocation.	Shear
Z-shape internal rotation	41°-43°	73°-75°	60°-63°	Delimited by fractures	0.17-42	Open	Cleavage lamellae displaying individual and random rotational movement.	Shear

Deformation intensity

Figure 9. Main morphological characteristics, geometric parameters, and deformation features of lamellae in kink bands formed parallel to the cleavage plane [001]

An analysis of the geometric and morphological features, combined with current models in the literature, suggests two key mechanisms for explaining the development of the six principal forms of kink bands: flexural slip strain and shear strain. In the case of flexural slip strain, the cleavage lamellae exhibit moderate to strong curvature without fractures along the kink band boundary (KBB). The thickness of the lamellae inside and outside the kink band zone (KBZ) remains unchanged; however, delamination cracks commonly occur at points of maximum curvature. These characteristics were widely observed in both sigmoidal-shape and S-shape kink bands.

Regarding shear strain, the translational and rotational accommodation movements of the cleavage lamellae along the kink band boundary (KBB) provide the most convincing evidence for this process. Two antagonistic forces operate simultaneously along the transverse surface of the mineral grain, causing the cleavage lamellae to break on both sides of the kink bands. A more comprehensive analysis of this mechanical behavior reveals four distinct domains, each with a unique natural strain pattern. For example, lenticular-shape kink bands exhibit elements similar to those found in a transtensional strain regime. The cleavage lamellae in the kink band zone (KBZ) adopt elongated rectangular shapes, with ends stretched near the KBB, and show interlamellar delamination cracks.

In contrast, Z-shape kink bands are characterized by a uniform KBZ width, parallel displacement along the cleavage plane, and moderate to relatively high rotation angles of the cleavage lamellae (Fig. 9). Similar to the observations reported by Plummer et al. (2021), although the presence of delamination cracks does not seem to affect the thickness of the cleavage lamellae, whether inside or outside the KBZ, the propagation of linear fractures along the KBB and the parallel displacement of the cleavage lamellae in the KBZ could only have occurred in a heterogeneous non-coaxial strain regime.

Regarding Z-shape internal dislocation and Z-shape internal rotation kink bands, and in accordance with the model proposed by Zhou et al. (2018), the development of these two deformation stages would have resulted from a significant increase in stress. Although there appears to be a minor random change in the kink band zone (KBZ) width after band formation in some cases, the most striking features of these kink bands are their exceptionally narrow band width, the nature of cleavage lamella movement, and the high angle β compared to other parameters (Fig. 9). From this perspective, the development of these kink bands is attributed to at least two different mechanisms. In one scenario, the zig-zag translational motion of atoms within the crystal lattice is clearly noticeable in the Z-shape internal dislocation kink bands, as evidenced by the domino-like sliding of the cleavage planes. In another scenario, the thin internal lamellae of Z-shape internal rotation kink bands exhibit random spin, resulting from an arbitrary rotation of a small part of the crystal lattice. In both scenarios, the rapid propagation of high stress likely caused the rupture of a small segment of the crystal lattice, leading to instability and the local formation of kink bands.

Given the wide variation in geometric parameters and the differing deformation patterns of cleavage lamellae within KBZs (Fig. 9), it can be inferred that the development of these microstructures was largely influenced by a transpressional deformation process. In this regime, deviatoric stress acted both parallel and obliquely to the cleavage plane. As suggested by Moreira and Dias (2022), the progressive internal strain within kink bands results from the accommodation of cleavage lamellae during layer shortening. The overall deformation pattern, characterized by a series of small parallelograms with discrete glide planes, indicates that the crystal lattices accommodated in response to an intense compressive stress regime.

6. Final Remarks

Apart from the explanations provided regarding the different kink bands present in mica grains, several aspects warrant attention:

1) Strain perpendicular to the [001] plane results in narrower, more elongated, and widely spaced kink bands, often accompanied by parallel planar fractures. These features indicate a higher level of localized deformation, where strain is efficiently accommodated within the bands, leading to distinctive geometry and spacing.
2) The occurrence of coplanar kink bands with two different orientations, perpendicular to the [001] plane, provides strong evidence of an abrupt change in the direction of the maximum principal stress over a short period. This phenomenon is indicative of a rapid, localized change in the stress regime.
3) Strain parallel to the [001] plane yields a wide variety of kink bands in terms of shape and size. The observed morphological differences are likely a result of varying local stress concentrations, which play a crucial role in shaping these bands.
4) Processes involving flexural sliding and shear strain offer reasonable explanations for the six different shapes identified. The primary mechanism of deformation in both cases is likely intracrystalline plasticity. Flexural sliding facilitates the accommodation of deformation within the crystal structure, allowing for the formation of various kink band geometries.
5) The magnitude of deformation observed in the cleavage lamellae for each kink band indicates different strain intensities. This variation in strain intensity is a key factor in determining the extent and nature of deformation within the mica grains.
6) Kink bands parallel to the [001] plane are significantly more frequent and diverse than those perpendicular to the [001] plane. This prevalence suggests that deformation along the [001] plane plays a critical role in the development of kink bands, likely due to the inherent crystallographic properties of mica.
7) The geometric parameters of kink bands appear to be more significantly influenced by the intensity of strain than by the formation mechanisms. Ultimately, the final geometry of the kink bands is determined by the intensity of the strain.

The pronounced internal deformation observed in the kink bands of the mica grains studied contrasts sharply with the kink bands documented in rocks subjected to tectonic deformation. Tectonic kink bands typically exhibit regular and well-defined patterns associated with persistent stress regimes (Dunham, 2010; Aller et al., 2020). In contrast, the kink bands analyzed in this study display morphological features indicative of a transient stress regime and a highly dynamic strain rate. This disparity in morphological features suggests a geological setting characterized by highly variable and dynamic stress conditions.

Notably, these morphological differences bear a remarkable similarity to the kink bands examined by Ebert et al. (2021) in the Chicxulub impact crater, which reflect deformation induced by shock waves. This observation reignites the debate about the potential use of kink bands as alternative evidence in impact cratering studies, as recently proposed by Stöffler et al. (2017) in their paper on a unified and updated shock metamorphism intensity determination system.

Acknowledgments

A number of generous colleagues contributed by reading and providing feedback during the preparation of this paper. We extend our gratitude to the colleagues at both institutions, EACH-USP and IG-IPA, for their invaluable assistance and support. W. Sallun Filho acknowledges the CNPq agency for providing a research grant. We also thank the anonymous referees whose comments significantly improved the quality of the manuscript. This study was supported by the Fapesp agency (Procs. 2011/50987-0 and 2012/50042-9).

Competing interests

The authors declare that they have no known competing financial interests or personal relationships that could have appeared to influence the work reported in this paper.

Informed consent

Obtained.

Ethics approval

The Publication Ethics Committee of the Canadian Center of Science and Education.

The journal's policies adhere to the Core Practices established by the Committee on Publication Ethics (COPE).

Provenance and peer review

Not commissioned; externally double-blind peer reviewed.

Data availability statement

The data that support the findings of this study are available on request from the corresponding author. The data are not publicly available due to privacy or ethical restrictions.

Data sharing statement

No additional data are available.

References

Anderson, E. K., Song, W. J., Johnson, S. E., & Cruz-Uribe, A. M. (2021). Mica kink band geometry as an indicator of coseismic dynamic loading. *Earth and Planetary Science Letters, 567*, 117000. https://doi.org/10.1016/j.epsl.2021.117000

Anderson, T. B. (1964). Kink bands and related geological structures. *Nature, 202*(4931), 272-274. https://doi.org/10.1038/202272a0

Aller, J., Bastida, F., & Bobillo-Ares, N. C. (2020). On the development of kink-bands: A case study in the Westasturian-Leonese Zone (Variscan belt, NW Spain). *Earth Science Bulletin, 191*(1), 6-10. https://doi.org/10.1051/bsgf/2020003

Becke, F. (1892). Petrographische Studien am Tonalit der Rieserferner. *Tschermaks Mineralogische und Petrographische Mitteilungen, 13*, 379-430. https://doi.org/10.1007/BF02996161

Bell, I. A., Wilson, C. J. L., McLaren, A. C., & Etheridge, M. A. (1986). Kinks in mica: Role of dislocations and (001) cleavage. *Tectonophysics, 127*(1-2), 49-65. https://doi.org/10.1016/0040-1951(86)90029-4

Christoffersen, R., & Kronenberg, A. K. (1993). Dislocation interactions in experimentally deformed biotite. *Journal of Structural Geology, 15*(9), 1077-1095. https://doi.org/10.1016/0191-8141(93)90117-6

Coutinho, J. M. V. (1980). *Mapa geológico da Grande São Paulo, 1:100.000*. Emplasa.

Deer, W. A., Howie, R. A., & Zussmann, J. (2013). *Introduction to the rock-forming minerals* (3rd ed.). The Mineralogical Society. https://doi.org/10.1180/DHZ

Dunham, R. E. (2010). Kink band development in the Darrington Phyllite on Samish Island, northwestern Washington. *WWU Graduate School Collection*, 66 p.

Dunham, R. E. (2010). *Kink band development in the Darrington Phyllite on Samish Island, northwestern Washington*. WWU Graduate School Collection. pp. 66.

Ebert, M., Poelchau, M. H., Kenkmann, T., Gulick, S. P. S., Hall, B., Lofi, L., McCall, N., & Rae, A. S. P. (2021). Comparison of stress orientation indicators in Chicxulub's peak ring: Kinked biotites, basal PDFs, and feather features. *Geological Society of America Special Papers, 550*, 479-493. https://doi.org/10.1130/2021.2550(22)

Etheridge, M. A., Hobbs, B. E., & Paterson, M. S. (1973). Experimental deformation of single crystals of biotite.

Contributions to Mineralogy and Petrology, 38, 21-36. https://doi.org/10.1007/BF00371741

Ferraris, G., & Ivaldi, G. (2002). Structural features of mica. *Reviews in Mineralogy and Geochemistry, 46*(1), 117-153. https://doi.org/10.2138/rmg.2002.46.05

French, B. M. (1998). Traces of Catastrophe: *A Handbook of Shock-Metamorphic Effects in Terrestrial Meteorite Impact Structures*. Lunar and Planetary Institute.

Hasui, Y., Carneiro, C. D. R., & Coimbra, A. M. (1975). The Ribeira folded belt. *Revista Brasileira de Geociências, 5*(4), 257-266. https://doi.org/10.25249/0375-7536.1975257266

Hörz, F., & Aherens, T. J. (1969). Deformation of experimentally shocked biotite. *American Journal of Science, 267*(9), 1213-1229. https://doi.org/10.2475/ajs.267.9.1213

Klein, C., & Hurlbut, C. S. (1993). *Manual of Mineralogy* (21st ed.). John Wiley & Sons.

Kollert, R., Björnberg, A., & Davino, A. (1961). Estudos preliminares de uma depressão circular na região de Colônia, Santo Amaro, São Paulo. *Boletim da Sociedade Brasileira de Geologia, 3*, 57-77.

Kronenberg, A. K., Kirby, S. H., & Pinkston, J. (1990). Basal slip and mechanical anisotropy of biotite. *Journal of Geophysical Research, 95*(B12), 19257-19278. https://doi.org/10.1029/JB095iB12p19257

Mares, V. M., & Kronenberg, A. K. (1993). Experimental deformation of muscovite. *Journal of Structural Geology, 15*(9-10), 1061-1075. https://doi.org/10.1016/0191-8141(93)90116-5

Melosh, H. J., & Ivanov, B. A. (1999). Impact cratering collapse. *Annual Review of Earth and Planetary Sciences, 27*, 385-415. https://doi.org/10.1146/annurev.earth.27.1.385

Misra, S., & Burg, J.-P. (2012). Mechanics of kink bands during torsion deformation of muscovite aggregate. *Tectonophysics, 548-549*, 22-33. https://doi.org/10.1016/j.tecto.2012.05.018

Moreira, N., & Dias, R. (2022). Accommodation structures during kink band evolution; quantitative methods applied to Late Variscan deformation of Portugal. *Journal of Structural Geology, 156*, 104550. https://doi.org/10.1016/j.jsg.2022.104550

Mügge, O. (1898). Über Translationen und verwandte Erscheinungen in Krystallen. *Neues Jahrbuch für Mineralogie, Geologie und Paläontologie, 1*, 71-158.

Osinski, G. R., & Pierazzo, E. (Eds.). (2012). *Impact Cratering: Processes and Products* (1st ed.). Wiley-Blackwell. https://doi.org/10.1002/9781118447307.ch1

Pimenta, S., Gutkin, R., Pinho, S. T., & Robinson, P. (2009). A micromechanical model for kink-band formation: Part II—Analytical modelling. *Composites Science and Technology, 69*(7-8), 956-964. https://doi.org/10.1016/j.compscitech.2008.07.024

Peterson, M. S., & Weiss, L. E. (1966). Experimental deformation and folding in phyllite. *Geological Society of America Bulletin, 77*(4), 343-374. https://doi.org/10.1130/0016-7606(1966)77[343:EDAFIP]2.0.CO;2

Plummer, G., Rathod, H., Srivastava, A., Radovic, M., Ouisse, T., Yildizhan, M., Persson, P. O. Å., Lambrinou, K., Barsoum, M. W., & Tucker, J. R. (2021). On the origin of kinking in layered crystalline solids. *Materials Today, 43*, 45-52. https://doi.org/10.1016/j.mattod.2020.11.016

Riccomini, C., Turcq, B. J., Ledru, M. P., Sant'Anna, L. G., & Ferrari, J. A. (2005). Cratera de Colônia, SP. Provável astroblema com registros do paleoclima quaternário na Grande São Paulo. In M. Winge, C. Schobbenhaus, M. Berbert-Born, E. T. Queiroz, D. A. Campos, & C. R. G. Souza (Eds.), *Sítios Geológicos e Arqueológicos do Brasil* (Vol. 2, pp. 35-44). CPRM/SIGEP.

Stöffler, D. (1966). Zones of impact metamorphism in the crystalline rocks of the Nördlinger Ries crater. *Contributions to Mineralogy and Petrology, 12*(1), 15-24. https://doi.org/10.1007/BF00370030

Stöffler, D., Hamann, C., & Metzler, K. (2017). Shock metamorphism of planetary silicate rocks and sediments: Proposal for an updated classification system. *Meteoritics & Planetary Science, 53*(1), 1-45. https://doi.org/10.1111/maps.12912

Turner, F. L. (1964). Analysis of kinks in mica of an Innsbruck mica schist. *Neues Jahrbuch für Mineralogie Monatshefte, 11*, 51-83.

Twiss, R. J., & Moores, E. M. (2007). Kinematic analysis of folds. In R. J. Twiss & E. M. Moores (Eds.), *Structural Geology* (pp. 363-398). W.H. Freeman and Company.

Verbeek, E. R. (1978). Kink-bands in the Somport slates, west-central Pyrenees, France and Spain. *Geological*

Society of America Bulletin, 89, 814-824. https://doi.org/10.1130/0016-7606(1978)89<814>2.0.CO;2

Velázquez, V. F., Gomes, C. B., Mansueto, M., Moraes, L. A. S., Sobrinho, J. M. A., Lucena, R. F., Sallun, A. E. M., & Sallun Filho, W. (2021). Morphological aspects, textural features and chemical composition of spherules from the Colônia impact crater, São Paulo, Brazil. *Solid Earth Sciences, 6*, 27-36. https://doi.org/10.1016/j.sesci.2020.12.004

Velázquez, V. F., Lucena, R. F., Azevedo Sobrinho, J. A., Martins Sallun, A. E. M., & Sallun Filho, W. (2018). Petrographic investigation of target rock transformation under high shock pressures from the Colônia impact crater, Brazil. *Earth Science Research, 7*(1), 13-24. https://doi.org/10.5539/esr.v7n1p13

Velázquez, V. F., Riccomini, C., Azevedo Sobrinho, J. M., Pletsch, M. A. J. S., Sallun, A. E. M., Sallun Filho, W., & Hachiro, J. (2013). Evidence of shock metamorphism effects in allochthonous breccia deposits from the Colônia crater, São Paulo, Brazil. *International Journal of Geosciences, 4*, 274-282. https://doi.org/10.4236/ijg.2013.41A025

Wadee, M. A., & Edmundus, R. (2005). Kink band propagation in layered structures. *Journal of the Mechanics and Physics of Solids, 53*, 2017-2035. https://doi.org/10.1016/j.jmps.2005.04.003

Zhou, L., Zhao, L., Liu, F., & Jang, J. (2018). A micromechanical model for longitudinal compressive failure in unidirectional fiber reinforced composite. *Results in Physics, 10*, 841-848. https://doi.org/10.1016/j.rinp.2018.07.030